Spherulitic Crystallization Behavior of Poly(ϵ-caprolactone) with a Wide Range of Molecular Weight

Hsin-Lung Chen,*,† Lain-Jong Li,‡ Wen-Chung Ou-Yang,§ Jenn Chiu Hwang,|| and Wen-Young Wong†

Department of Chemical Engineering, Chang Gung College of Medicine and Technology, Kwei-San, Taoyuan, Taiwan, R. O. C., Department of Chemistry, National Taiwan University, Taipei, Taiwan, R. O. C., Department of Chemical Engineering, National Kaohsiung Institute of Technology, Kaohsiung, Taiwan, R. O. C., and Department of Chemical Engineering, Yuan Ze Institute of Technology, Nei-Li, Taoyuan, Taiwan, R. O. C.

Received May 7, 1996; Revised Manuscript Received November 20, 1996[⊗]

ABSTRACT: Poly(ϵ-caprolactone) (PCL) with a wide range of molecular weight (MW) has been prepared via fractionation by either precipitating PCL/chloroform solutions into different amounts of methanol or adding methanol into PCL/tetrahydrofuran (THF) solutions. The samples with M_n ranging from 1900 to 64 700 were used to investigate the MW effects on the spherulite growth rate, nucleation density, and equilibrium melting point (T_m^0) of PCL. The variation of spherulite growth rate with MW exhibited a maximum rather than a conventional monotonic drop. The existence of such a maximum was rationalized by considering the interplay between the effects of MW on T_m^0 and segmental mobility. A growth kinetic formula proposed by Hoffman was employed to extract the crystal surface free energy product ($\sigma\sigma_e$). In contrast to the conventional Lauritzen−Hoffman analysis which was based on the growth rates measured at different crystallization temperatures (T_c) for a given MW, the present analysis was based on the growth rates measured for different MW at a given T_c. The spherulite nucleation density was found to be higher for the sample with larger MW, and this observation was interpreted based on the individual effects of MW on the primary nucleation rate and spherulite growth rate. An increase in MW promoted the nucleation rate much more significantly compared with its effect on the growth rate, and this in turn led to a higher nucleation density. An unusual morphology due to the segregation of uncrystallizable short chains into the interfibrillar regions of the spherulites was also observed for PCL with $M_n = 1900$.

Introduction

Molecular weight (MW) is one of the key variables governing the thermodynamic and kinetic parameters of polymer crystallization. The equilibrium melting point (T_m^0), crystal thickness, crystallization kinetics, degree of crystallinity, and crystalline morphology may all be influenced by MW.[1−13] T_m^0 was found to increase with increasing MW, owing to the lower entropy of melting associated with longer chains.[5,12−13] Crystallization rate, on the other hand, generally decreased with increasing MW because of the lower segmental mobility associated with longer chains.[6]

Poly(ϵ-caprolactone) (PCL) is a crystalline and biodegradable polyester with a glass transition temperature (T_g) of ca. −60 °C and an observed melting point around 55 °C. Extensive studies of PCL and its blends have been reported.[9,15−23] In one of the studies,[23] Cheung dissolved a PCL in chloroform followed by precipitating it into methanol. Interestingly, the MW of the recovered PCL precipitate was found to be appreciably higher than that of the as-received sample. This observation suggested that a strong MW fractionation occurred during precipitation, and one must be aware of such a MW shift when using solution precipitation to prepare the blends of PCL or to purify this polymer.

Since fractionation may be affected significantly by the condition under which the precipitation was conducted, it will be of interest to prepare PCL with a wide range of MW by various precipitation procedures, and the samples thus obtained will be useful for investigating the MW effect on the structure and properties of this polymer. The MW effect on the crystallization behavior of PCL has been reported previously by Philips et al.[9] The samples with three different MW (M_w = 7000, 15 000, and 40 000) were investigated in that study. In the present investigation, the MW effect on the crystallization behavior of PCL using samples with a broader MW range was reported. PCL with MW ranging from M_n = 1900 to 64 700 were prepared by either precipitating PCL/chloroform solution into different amount of methanol or adding methanol into PCL/tetrahydrofuran (THF) solutions. The effects of MW on the spherulite growth kinetics, nucleation density, and T_m^0 will be critically discussed in this paper.

Table 1. MW and Sources of the Four as-Received PCL Samples

sample	M_n	M_w	source
PCLA	44 700	59 100	Solvay Interox
PCLB	55 800	71 900	Solvay Interox
PCLC	22 400	46 100	Aldrich
PCLL	2 800	3 800	Yun Jian Polymer

Experimental Section

Four commercial PCL samples were used as the starting materials for MW fractionation. The MW and the sources of these four materials are tabulated in Table 1. The fractionations were carried out by either precipitating 4 wt % PCL/chloroform solutions into different amounts of methanol or by adding methanol into 10 wt % PCL/THF solutions. Table 2 lists the preparation procedures of several PCL samples along with their M_n and M_w. All dissolution and precipitation were conducted at room temperature.

The absolute molecular weight of PCL was determined by a Kratos Model Spectraflow 400 gel permeation chromatograph

* To whom correspondence should be addressed.
† Chang Gung College of Medicine and Technology.
‡ National Taiwan University.
§ National Kaohsiung Institute of Technology.
|| Yuan Ze Institute of Technology.
⊗ Abstract published in *Advance ACS Abstracts,* February 15, 1997.

S0024-9297(96)00673-0 CCC: $14.00

Table 2. M_n, M_w, and Preparation Procedures of Selective PCL Samples

sample	M_n	M_w	preparation procedure
1	6700	7800	poured PCLL/chloroform solution into 10-fold excess volume of methanol
2	6300	7300	poured PCLL/chloroform solution into 50-fold excess volume of methanol
3	2700	4400	after sample 2 was filtered out, the remaining solution was dried using a rotatory evaporator at 50 °C
4	4400	5700	poured sample 3/chloroform solution into 50-fold excess volume of methanol
5	1900	3300	after sample 4 was filtered out, the remaining solution was dried using a rotatory evaporator at 50 °C
6	64700	77600	precipitated by adding one-third volume of methanol into PCLB/THF solution
7	19600	39200	after sample 6 was filtered out, one-third volume of methanol was added into the remaining solution

(GPC) equipped with Shodex KF-801, KF-802, KF-803, and KF-804 columns and Viscotek Model-100 differential refractometer/viscometer detectors. The average molecular weights (M_n, M_w, and M_z) were obtained through the universal calibration curve using the Viscotek Unical GPC software version 4.01. The spherulite growth and morphology of PCL with different MW were monitored with an Olympus BH-651P polarized optical microscope. The PCL powder was first melted on a Linkam TP92 hot stage at 80 °C for 3 min. The sample was then quickly transferred to another hot stage equilibrated at the desired crystallization temperature (T_c) and the spherulite growth was monitored. Micrographs were taken at intervals for measuring the spherulite radii at various time periods. The growth rate was calculated from the change of spherulite radius with time, dR/dt. Melting point measurement was performed with a Perkin-Elmer DSC 7. The PCL samples were heated to 80 °C followed by annealing for 3 min to erase previous thermal history. The samples were subsequently cooled at ca. 160 °C/min to the desired T_c. After crystallizing for 11 h, the samples were scanned from room temperature at 20 °C/min to record the melting endotherms. The peak temperature of the endotherm was considered as the melting point of the sample.

Results and Discussion

In this study, PCL with a wide range of MW was prepared by precipitating PCL/chloroform solution into different amounts of methanol nonsolvent or by adding methanol into PCL/THF solutions. Figure 1 shows the GPC curves of the as-received PCLL and the PCL prepared by precipitating PCLL/chloroform solution into different amount of methanol. The curves shift toward shorter elution time after precipitation, indicating that fractionation did take place during precipitation. The dependence of MW on the volume ratio of polymer solution to methanol was not identified here, because no attempt was made to precisely control the precipitation condition such as the temperature and the process of pouring the polymer solutions into methanol. Table 2 lists some examples of the procedures for preparing the PCL with different MW. The lowest and highest M_n values of PCL prepared in this study were 1900 and 64 700, respectively.

Table 2 demonstrated that PCL with a wide range of MW can be obtained by precipitation under different conditions. The samples thus prepared will then be useful for investigating the MW effect on the crystallization behavior of this polymer. The MW effect on the growth rate (G) of PCL spherulites was evaluated first. The plot of ln G vs ln X_n (X_n is the degree of polymerization) is displayed in Figure 2. It is seen that, in contrast to the conventional observation, the variation

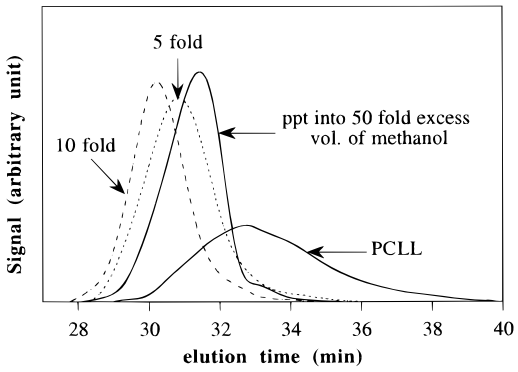

Figure 1. GPC curves of PCL prepared by precipitating PCLL/chloroform solutions into different amounts of methanol indicated in the figure. The curves shift toward the left after precipitation, showing that fractionation did take place during precipitation.

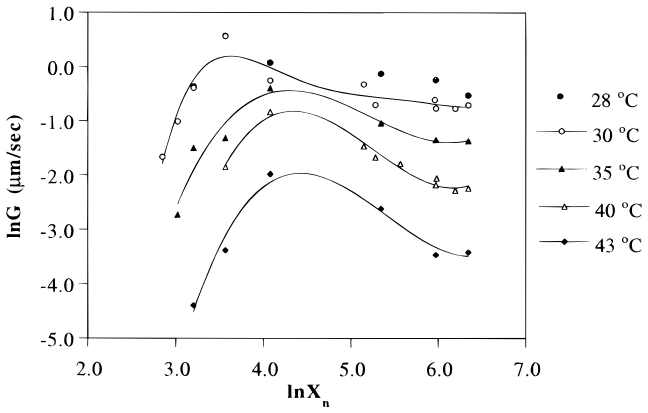

Figure 2. Variation of spherulite growth rate with degree of polymerization of PCL. The variation exhibits a maximum rather than a monotonic drop.

of growth rate with MW exhibits a maximum rather than a monotonic drop. The existence of such a maximum may be rationalized if the effect of MW on, besides the segmental mobility, T_m^0 is also taken into account. Because increasing MW would raise T_m^0, this means that at a given T_c the sample with higher MW was indeed undergoing crystallization at a larger degree of supercooling or with a larger driving force. Combined with the influence on segmental mobility, it can be concluded that increasing MW should exert two opposing effects on the crystallization rate of a polymer; one is to reduce the segmental mobility, which would result in retardation of crystallization rate, while the other is to increase the degree of supercooling, which would promote the crystallization rate. The interplay between these two will determine the observed growth rate and may then generate a maximum in the growth rate−MW plot as that observed in Figure 2. For the low MW regime, the effect of T_m^0 increase was more pronounced than the reduction in segmental mobility, and thus the growth rate increased with increasing MW; the opposite was true for the high MW regime.

The MW effect on segmental mobility has been incorporated into the growth rate formula by Hoffman by considering the role of reptation in crystallization. This treatment gives the growth rate as[6]

$$G = \left(\frac{K}{n}\right)\exp\left(\frac{Q_D^*}{RT_c}\right)\exp\left[-\frac{\alpha b_0 \sigma \sigma_e T_m^0(n)}{k_B \Delta H_f^\circ T_c [T_m^0(n) - T_c]}\right] \quad (1)$$

where n is the average number of units in a polymer

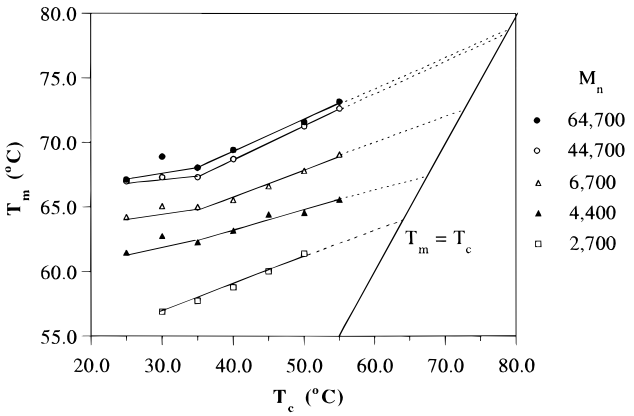

Figure 3. Hoffman−Weeks plot of PCL with various MW.

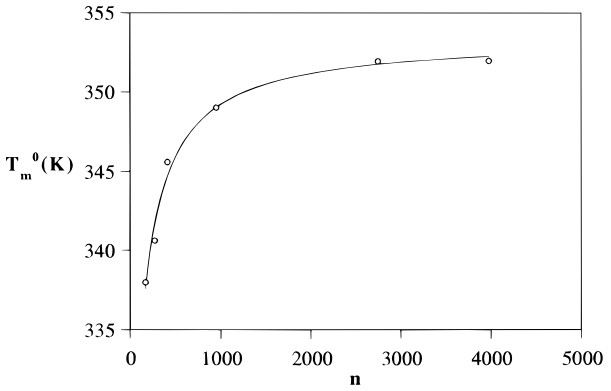

Figure 4. Variation of T_m^0 with MW of PCL. The curve represents the fit by eq 5.

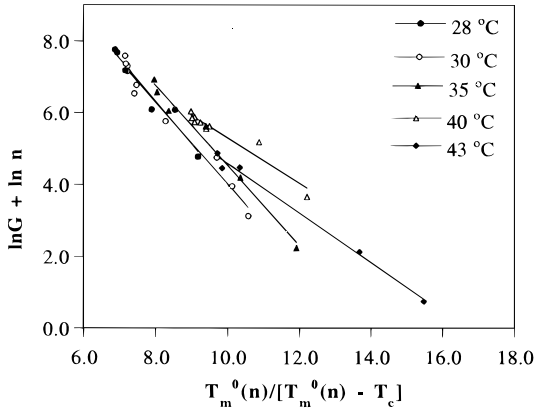

Figure 5. The plot of ln G + ln n_n vs $T_m^0(n)/[T_m^0(n) - T_c]$.

chain, K is a constant depending on the growth regime, Q_D^* is the activation energy for the reptation process, σ and σ_e are the side and fold surface free energy, respectively, b_0 is the monomolecular thickness, $\Delta H_f°$ is the bulk enthalpy of melting per unit volume of crystal, and α is a constant depending on the growth regime. T_m^0 in eq 1 is expressed with parentheses, $T_m^0(n)$, to denote that T_m^0 is a function of n. Assuming that the surface free energies are weak functions of MW, eq 1 can be rearranged to give

$$\ln G + \ln n = \ln W(T_c) - \psi(T_c)\frac{T_m^0(n)}{T_m^0(n) - T_c} \quad (2)$$

where

$$\ln W(T_c) = \ln K - \frac{Q_D^*}{RT_c} \quad (3)$$

and

$$\psi(T_c) = \frac{\alpha b_0 \sigma \sigma_e}{k_B \Delta H_f° T_c} \quad (4)$$

Equation 2 indicates that a plot of ln G + ln n vs $T_m^0(n)/[T_m^0(n) - T_c]$ for a given T_c would yield a straight line with the slope of $-\psi(T_c)$. Of course, this is true only if the spherulite growth for the MW range investigated takes place within one regime since $\psi(T_c)$ depends on the value of α. Deviation from a single linearity would occur if the samples under investigation span more than one growth regime at a given T_c. It follows that if $\psi(T_c)$ is determined, the surface free energy product $\sigma\sigma_e$ can then be calculated from eq 4. This provides an alternative method to extract the crystal surface free energy based on the growth rate analysis. In contrast to the conventional method which analyzes the growth rates measured at different T_c for a fixed MW, this method analyzes the growth rates measured for different MW at a given T_c.

The analysis using eq 2 to determine $\sigma\sigma_e$ for PCL was performed here. The average number of units was calculated by $n = M_n/M_u$ with M_u taken as 114 ÷ 7 g/mol, because a caprolactone unit [−$(CH_2)_5$COO−] has the molecular weight of 114 and is considered to contain seven units.

Analysis of eq 2 also requires the knowledge of $T_m^0(n)$. The T_m^0s of PCL corresponding to different MW were extrapolated by the Hoffman−Weeks plot in Figure 3. As expected, PCL with a higher MW has a higher T_m^0. The extrapolated T_m^0 for the two high MW samples (M_n = 44 700 and 64 700) was 78.9 °C; this value is 2.6 °C higher than that reported by Vion et al.[18] and about 8 °C higher than that reported by Philips et al.[9] and by Jonza and Porter.[15] The variation of T_m^0 with n is shown in Figure 4. The $T_m^0(n)$−n relationship can be described by the following relationship[24]

$$T_m^0(n) = T_m^0(\infty)\frac{(a + n)}{(b + n)} \quad (5)$$

with a = 118.9, b = 132.3, and $T_m^0(\infty)$ = 353.0 K. Substituting eq 5 for the $T_m^0(n)$ in eq 2, the plot of ln G + ln n vs $T_m^0(n)/[T_m^0(n) - T_c]$ can then be constructed, as displayed in Figure 5. The plot appears linear over the entire MW range for the T_cs investigated, which would indicate that the growth regime remains virtually the same over the MW range. It is noted that two different slopes can be identified among the linear lines in Figure 5. The slopes for T_c = 28, 30, and 35 °C are about the same but are larger than that for T_c = 40 and 43 °C. The slope of the line for T_c = 40 °C is −0.63, while that for T_c = 30 °C is −1.14, which is 1.8 times that for T_c = 40 °C. Table 3 tabulates the values of $\psi(T_c)$ obtained for different T_cs. Equation 4 prescribes that the slope $-\psi(T_c)$ is proportional to the constant α whose value is determined by the growth regime; α = 4 for regime I and III while α = 2 for regime II.[25,26] Therefore, the different $\psi(T_c)$ observed in Figure 5 can be

Table 3. The values of $\psi(T_c)$ and $\sigma\sigma_e$ Obtained in the Analysis

	T_c (°C)				
	28	30	35	40	43
$\psi(T_c)$	1.19	1.14	1.12	0.63	0.68
$\sigma\sigma_e$ (erg^2/cm^4)	445	425	418	487	525

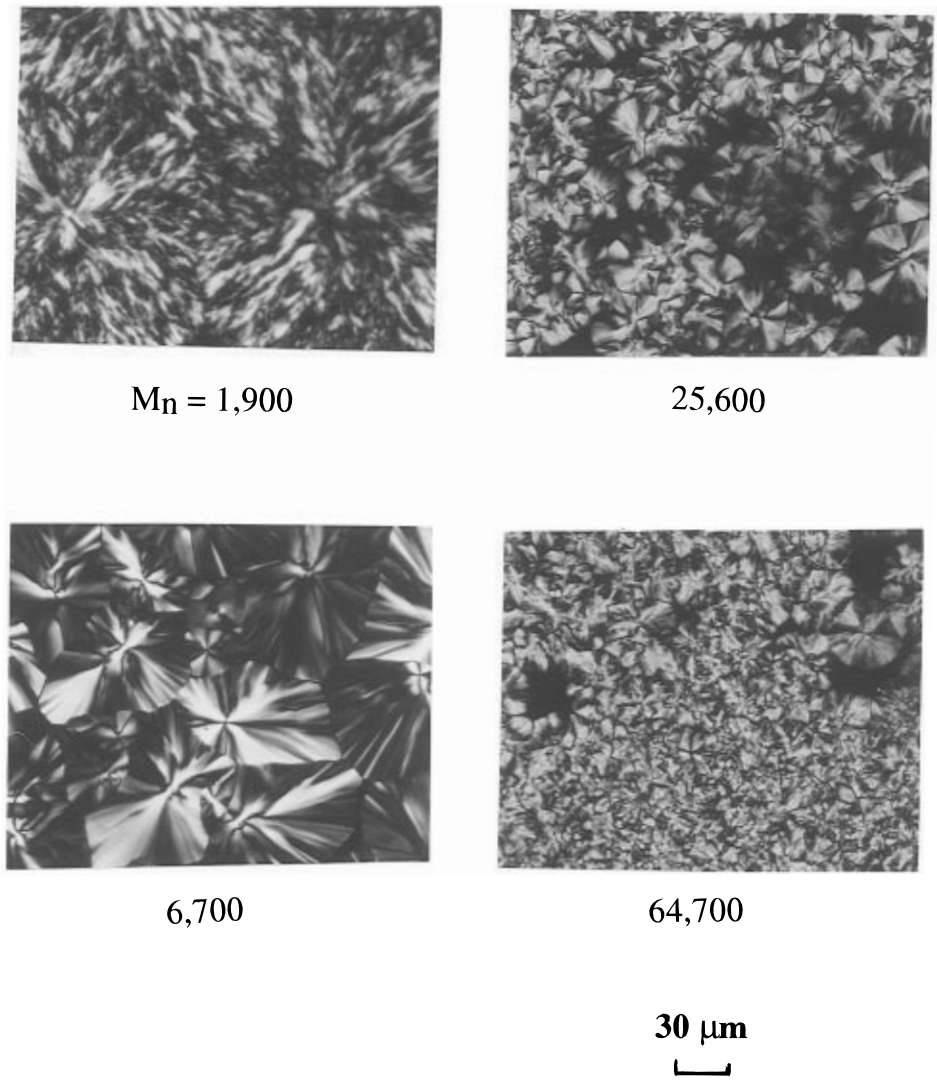

Figure 6. Spherulites viewed under polarized optical microscopy for PCL with various M_n indicated in the figure (T_c = 40 °C). The nucleation density is found to increase with increasing MW.

attributed to the different regimes that the spherulite growth was associated with. The growth took place in regime II at 40 and 43 °C, whereas it proceeded in regime III at 28, 30, and 35 °C, and as a result, $\psi(T_c)$ for 30 °C is about 2 times that for 40 °C. Using the Lauritzen *Z* test, Goulet and Prud'homme suggested that the growth of PCL spherulites in the T_c range from 25 to 45 °C was located in regime II.[19] Nevertheless, the results presented here suggested that the PCL spherulite growth below 35 °C occurred in regime III.

Using the values of b_0 = 4.13 Å and $\Delta H_f°$ = 1.48 × 10^9 erg/cm^3, the surface free energy product $\sigma\sigma_e$ was calculated on the basis of regime III (below 35 °C) and regime II growth (above 35 °C). The results are also listed in Table 3. The average value of the calculated $\sigma\sigma_e$ is 460 erg^2/cm^4.

The effect of MW on the nucleation density of PCL spherulites is also evaluated by comparing the size of spherulites after impingement. Figure 6 shows the spherulites viewed under polarized optical microscopy for PCL with various MW. Apparently, the spherulite size decreased drastically with increasing MW, or the nucleation density increased with increasing MW.

The average size of spherulites or the nucleation density can be thought to be determined by the competition between the rates of nucleation and subsequent growth of the spherulites. The faster the nucleation, the smaller the spherulites that will be formed after impingement and thus the higher the nucleation density that will be observed. Therefore, in order to understand the MW effect on the nucleation density, the respective effects of MW on the rates of nucleation and growth must be considered first.

For the sake of simplicity, if the nucleation can be approximated as a homogeneous primary nucleation, the rate of nucleation can then be written as[13]

$$i \propto \frac{1}{n} \exp\left\{-\frac{32\sigma^2\sigma_e T_m^0(n)^2}{k_B T_c(\Delta H_f°)^2[T_m^0(n) - T_c]^2}\right\} \qquad (6)$$

The preexponential factor, 1/*n*, is to take account of the MW effect on the reptation in the nucleation, assuming the reptation in this process is approximately the same as that in crystal growth. From eq 1, the growth rate is now written as

$$G \propto \frac{1}{n} \exp\left\{-\frac{2\sigma\sigma_e b_0 T_m^0(n)}{k_B T_c \Delta H_f°[T_m^0(n) - T_c]}\right\} \qquad (7)$$

for regime II growth. Comparing eqs 6 and 7, it can be seen that the primary nucleation rate varies with exp[−$1/(T_m^0 - T_c)^2$] while the growth rate varies with exp[−

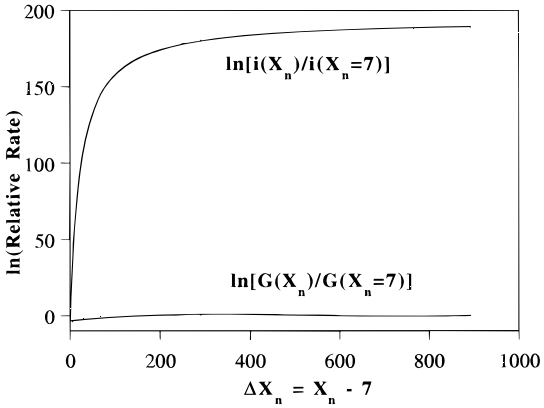

Figure 7. Relative changes of nucleation and growth rate as the degree of polymerization of PCL is increased from 7. The nucleation rate was promoted much more significantly compared with the growth rate.

$1/(T_m^0 - T_c)]$. This means that the primary nucleation rate is more susceptible to the change in the degree of supercooling than the growth rate. In other words, as the crystallization temperature is lowered, the rate of primary nucleation will be promoted to a larger extent than that of crystal growth, and as a result, the nucleation density increases with decreasing T_c.

MW can also affect the degree of supercooling due to its influence on T_m^0. Because of higher T_m^0, polymer with larger M_n actually crystallized with a larger degree of supercooling at a given T_c and thus would have a higher nucleation density. A calculation is performed here to compare the individual effects of MW on the nucleation and growth rates at $T_c = 40$ °C. From eqs 6 and 7, the ratios $\ln[i(X_n)/i(X_n=7)]$ and $\ln[G(X_n)/G(X_n=7)]$ were calculated. These ratios reflect the relative changes of nucleation and growth rate as X_n was increased from 7. The calculated results were plotted against $\Delta X_n = X_n - 7$ in Figure 7. Apparently, an increase in MW promoted the nucleation rate in a much more significant fashion compared with its effect on the growth rate, and as a consequence, a significant increase in nucleation density is expected.

It is also noted in Figure 6 that the sample with $M_n = 1900$ displays a spherulite morphology which is distinctly different from that of the samples with higher MW. For the samples with higher M_n, the spherulite texture is basically compact, while on the other hand, the PCL with $M_n = 1900$ exhibits a coarse spherulite texture with distinguishable branches in the spherulites. This unusual morphology can be ascribed to the segregation of the uncrystallizable short chains during the crystallization process. The PCL with $M_n = 1900$ has the polydispersity index of 1.7, which is relatively high compared with other PCL samples; upon crystallization at 40 °C, there may exist the short PCL chains that are not crystallizable because their equilibrium melting points are close to or even lower than 40 °C. These short chains must then be rejected away from the crystal growth front. Depending on the distance of rejection, they may be trapped in the crystalline interlamellar zones, in the interfibrillar regions of the spherulites, or in the interspherulitic regions.[27] The morphology observed in Figure 6 indicated that the uncrystallizable species should be segregated predominantly to the interfibrillar regions where the uncrystallizable chains were trapped between the branches of the spherulites.

Conclusions

It is demonstrated in this study that PCL exhibited a strong MW fractionation on precipitation. The MW dependence of spherulite growth rate displayed a maximum which was attributable to the interplay between two opposing effects associated with the influence of MW on T_m^0 and segmental mobility. A method based on the analysis of growth rates for different MW at a given T_c was also proposed to extract the crystal surface free energy product. The nucleation density of PCL spherulites was found to increase prominently with increasing MW, and this can be interpreted based on the respective effects of MW on the rates of nucleation and growth. An unusual morphology with distinct branches in the spherulites was observed for PCL with $M_n = 1900$. This morphology was due to the segregation of the uncrystallizable chains into the interfibrillar regions in the spherulites.

References and Notes

(1) Magill, J. H. *J. Appl. Phys.* **1964**, *35*, 3249.
(2) Mandelkern, L.; Allou, Jr. A. L.; Gopalan, M. *J. Phys. Chem.* **1968**, *72*, 309.
(3) Mandelkern, L. *J. Phys. Chem.* **1971**, *75*, 3920.
(4) Ergoz, E. Fatou, J. G.; Mandelkern, L. *Macromolecules* **1972**, *5*, 147.
(5) Wunderlich, B.; Czornyj, G. *Macromolecules* **1977**, *10*, 906.
(6) Hoffman, J. D. *Polymer* **1982**, *23*, 656.
(7) Mandelkern, L. *Polym. J.* **1985**, *17*, 337.
(8) Lovinger, A. J.; Davis, D. D.; Padden, F. J., Jr. *Polymer* **1985**, *26*, 1595.
(9) Philips, P. J.; Rensch, G. J.; Taylor, K. D. *J. Polym. Sci. Part B: Polym. Phys.* **1987**, *25*, 1725.
(10) Day, M. ; Deslandes, Y.; Roovers, J.; Suprunchuk, T. *Polymer* **1991**, *32*, 1258.
(11) Deslandes, Y.; Sabir, F.-N.; Roovers, J. *Polymer* **1991**, *32*, 1267.
(12) Wunderlich, B. *Macromolecular Physics*; Academic Press: New York, 1977; Vol. 2.
(13) Schultz, J. M. *Polymer Materials Science*; Prentice-Hall: Englewood Cliffs, 1974.
(14) Crescenzi, V.; Manzini, G.; Galzolzri, G.; Borri, C. *Europ. Polym. J.* **1972**, *8*, 449.
(15) Jonza, J. M.; Porter, R. S. *Macromolecules* **1986**, *19*, 1946.
(16) Nojima, S.; Tsutsui, H.; Urushihara, M.; Kosaka, W.; Kato, N.; Ahida, T. *Polym. J.* **1986**, *8*, 451.
(17) Chynoweth, K. R.; Stachurski, Z. H. *Polymer* **1986**, *27*, 1912.
(18) Vion, J. M.; J'erome, R.; Teyssie', P.; Aubin, M.; Prud'homme, R. E. *Macromolecules* **1986**, *19*, 1828.
(19) Goulet, L.; Prud'homme, R. E. *J. Polym. Sci. Part B: Polym. Phys.* **1990**, *28*, 2329.
(20) Goh, S. H.; Neo, M. K. *Eur. Polym. J.* **1991**, *9*, 927.
(21) Cheung, Y. W.; Stein, R. S. *Macromolecules* **1994**, *27*, 2512.
(22) Oudhuis, A. A. C. M.; Thiewes, H. J.; van Hutten, P. F.; ten Brinke, G. *Polymer* **1994**, *35*, 3936.
(23) Cheung, Y. W. Ph.D. Thesis, University of Massachuesetts, Amherst, MA, 1994.
(24) Huggins, M. L. *J. Phys. Chem.* **1939**, *43*, 1083.
(25) Hoffman, J. D.; Davis, G. T.; Lauritzen, J. I., Jr. In *Treatise on Solid State Chemistry*; Hanny, N. B. Ed; Plenum Press: New York, 1976; Chapter 7.
(26) Hoffman, J. D. *Polymer* **1983**, *24*, 3.
(27) Grevecoeur, G.; Groeninckx, G. *Macromolecules* **1991**, *24*, 1190.

MA960673V